International Research Journal of Engineering and Technology (IRJET) e-ISSN: 2395-0056
Volume: 13 Issue: 03 | Mar 2026 www.irjet.net p-ISSN: 2395-0072

Design and Experimental Validation of an IoT-Enabled Residential Automatic Power Factor Correction System

Pradeep. S[1], Nikitha. S[2], Shivani. S[3], Mamatha. T[4], Charan. N[5], Mr.Ramesh Babu. S[6]

[1,2,3,4,5] *B.Tech Students, Department of Electrical and Electronics Engineering*
[6] *Assistant Professor, Department of Electrical and Electronics Engineering*
Nalla Malla Reddy Engineering College , Hyderabad, India

Abstract - – *Uncompensated reactive power in low-voltage residential distribution networks contributes to elevated feeder I^2R losses, reduced line capacity, and degraded voltage regulation — issues that become increasingly significant as residential load density grows. While distributed Automatic Power Factor Correction (APFC) systems offer a practical solution, existing prototypes typically rely on pre-programmed or manually calibrated capacitor values, limiting their accessibility and accuracy in practical non-technical deployments. This paper presents the design and experimental validation of a low-cost, IoT-enabled residential APFC prototype utilizing an ESP32 microcontroller, a PZEM-004T v4.0 energy monitoring module, and a six-step relay-switched capacitor bank rated at 440 V AC. A key contribution of the proposed system is an automated capacitor characterization mode that measures and stores each capacitor's actual reactive power contribution under live supply conditions, eliminating manual calibration and enabling consumer-friendly plug-and-play operation. Real-time IoT monitoring is implemented via MQTT communication through the HiveMQ cloud broker, with electrical parameters displayed locally on a 20×4 LCD and remotely via the Electrical Parameter Monitor (EPM) mobile application developed on the MIT App Inventor platform. Experimental validation under resistive and inductive load conditions confirmed correct compensation logic and effective stepwise power factor improvement. Under an R-L test load, the system improved power factor from 0.71 to 0.97, reduced reactive power demand from 141 VAR to 29 VAR, and achieved an estimated 46.4% reduction in feeder resistive losses — with experimental results closely corroborating theoretical predictions. The proposed system demonstrates the viability of self-calibrating, IoT-integrated distributed APFC for smart grid and Advanced Metering Infrastructure compatible residential applications.*

Key Words: **Automatic Power Factor Correction; Reactive Power Compensation; ESP32; Internet of Things; Smart Grid; MQTT.**

I .INTRODUCTION

Reactive power compensation is critical for maintaining voltage stability and minimizing I^2R losses in low-voltage residential distribution networks. While individual household reactive demand is modest, its aggregate effect across feeders and substations is substantial—contributing to elevated conductor losses, reduced line capacity, and accelerated equipment aging [1], [3]. Centralized compensation via substation capacitor banks addresses broad voltage regulation but lacks the granularity to respond to localized or rapidly varying reactive demands introduced by modern distributed energy resources (DERs) and dynamic load profiles [2], [4].

Distributed Automatic Power Factor Correction (APFC) systems—deployed at the load level—offer a practical alternative by compensating reactive power at its source through relay-switched capacitor banks controlled by low-cost microcontrollers [5]. Concurrently, Internet of Things (IoT) integration via lightweight MQTT messaging over cloud brokers such as HiveMQ enables real-time monitoring of electrical parameters, providing both utilities and consumers with actionable grid data [2], [6]. Although inverter-based distributed energy resources can provide dynamic reactive support, relay-switched capacitor solutions remain more cost-effective and universally deployable across diverse residential settings [7].

This paper presents the design and experimental validation of an IoT-enabled residential APFC prototype using a PZEM-004T energy measurement module, an ESP32 microcontroller, and a six-step relay-controlled capacitor bank. The system incorporates real-time MQTT communication via HiveMQ, a 20×4 LCD display for local feedback, and a custom mobile application for remote monitoring. Experimental results confirm effective power factor improvement from 0.71 to 0.97 under inductive loading, demonstrating the viability of distributed load-level compensation for residential smart grid applications.

II. LITERATURE REVIEW

A.Distributed vs. Centralized Reactive Power Compensation

Reactive power management is fundamental to voltage stability, loss minimization, and asset utilization in distribution networks [1], [3]. Centralized compensation—typically via substation capacitor banks or voltage regulators—addresses broad voltage regulation but is increasingly insufficient for modern grids with dynamic loads and high distributed energy resource (DER) penetration [2]. Such schemes lack the granularity to

respond rapidly to localized reactive demand fluctuations, particularly over long low-voltage feeders where reactive power transmits poorly [3], [5].

Distributed APFC systems overcome these limitations by deploying small compensators close to end-use loads, operating autonomously through relay-switched capacitor banks controlled by microcontrollers such as the ESP32 [5]. Analytical models confirm that distributed control outperforms centralized methods in radial residential networks, achieving superior feeder loss reduction, improved bus voltage profiles, and greater scalability [1], [4].

B. Aggregated Impact on Feeders and Transformers

Although individual residential reactive demands are modest, their cumulative effect across feeders and substations is significant—up to 70% of total system losses occur within distribution networks, with approximately 13% of delivered energy dissipated as heat from uncompensated reactive currents [3], [4]. Coordinated deployment of distributed APFC at neighborhood scale can substantially reduce feeder loading, free line capacity, and extend transformer lifespan through reduced thermal stress [4], [5].

A. IoT Monitoring and Advanced Metering Infrastructure

The proliferation of IoT and Advanced Metering Infrastructure (AMI) technologies has enabled real-time acquisition and wireless communication of key electrical parameters using lightweight publish-subscribe protocols such as MQTT over cloud brokers like HiveMQ [2], [6]. Integrating IoT monitoring with APFC hardware—combining PZEM-004T measurement modules, ESP32 microcontrollers, and mobile application interfaces—provides utilities with granular grid visibility and empowers consumers with actionable power quality data [6].

B. Research Gaps

Inverter-based DERs offer fast dynamic reactive support but remain constrained by cost and regulatory barriers; relay-switched capacitor banks are therefore more universally applicable for residential compensation [7]. Despite demonstrated technical and economic benefits, significant gaps remain: large-scale field validation of aggregated feeder impacts is scarce; optimal coordination between distributed controllers and existing AMI infrastructure requires further study; and cybersecurity implications of pervasive IoT deployment in distribution systems have not been fully addressed. The present work contributes toward bridging the first gap through experimental prototype validation.

III. SYSTEM ARCHITECTURE AND METHODOLOGY

A.System Overview

The proposed system performs real-time reactive power compensation at the residential load level and enables remote monitoring through wireless communication. As shown in Fig. 1, the architecture integrates five functional units: electrical parameter measurement, central processing and control, capacitor switching, user interface, and IoT communication. The ESP32 DevKit V1 serves as the central processing unit, executing the compensation algorithm, managing relay switching, storing calibration data in non-volatile memory, and handling Wi-Fi-based MQTT communication.

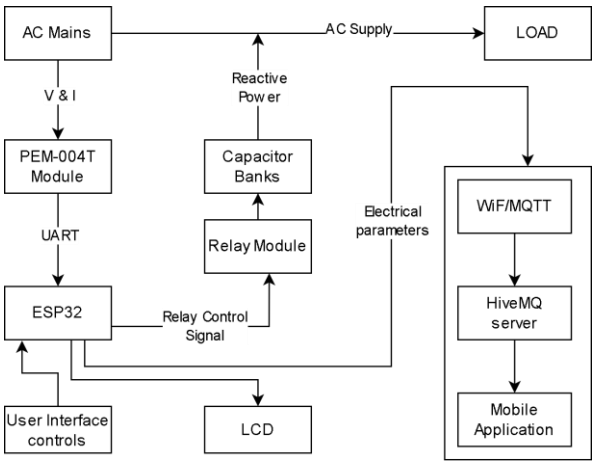

Fig. 1. Block diagram of the proposed IoT-enabled APFC system.

B. Electrical Parameter Measurement

Electrical parameters are measured using a PZEM-004T v4.0 energy monitoring module coupled with a 100 A solid-core current transformer (2000:1 ratio), providing galvanic isolation between the high-voltage AC line and the low-voltage control circuitry. The module directly computes RMS voltage, RMS current, active power, reactive power, and power factor, transmitting all values to the ESP32 via UART serial communication for use as inputs to the compensation algorithm.

C. Capacitor Switching Network

Reactive power compensation is implemented using a six-step capacitor bank (R1 = 5.0 µF, R2–R4 = 2.5 µF each, R5–R6 = 1.5 µF each), with each capacitor individually controlled by a relay module rated at 10 A / 250 VAC. The reactive power supplied by each capacitor is given by $Qc = V^2 \cdot 2\pi f \cdot C$, where V is RMS voltage, f is supply frequency, and C is capacitance. A 30 A load relay provides isolation during calibration, and a 120 kΩ discharge resistor across each

capacitor ensures safe charge dissipation upon disconnection.

D. Control Algorithm

The control flowchart is presented in Fig. 2. The ESP32 continuously acquires electrical parameters and evaluates the power factor against a threshold of 0.95. If compensation is required, the controller calculates the reactive demand deficit and selects the capacitor step whose stored VAR contribution is closest to the required compensation. After each switching action, parameters are re-evaluated to confirm adequate correction. Overcompensation is prevented by verifying that activating the next step would not result in a leading power factor condition. A dedicated capacitor characterization mode individually energizes each capacitor, measures its actual reactive contribution, and stores the value in non-volatile memory compensating for manufacturing tolerances and supply voltage variations.

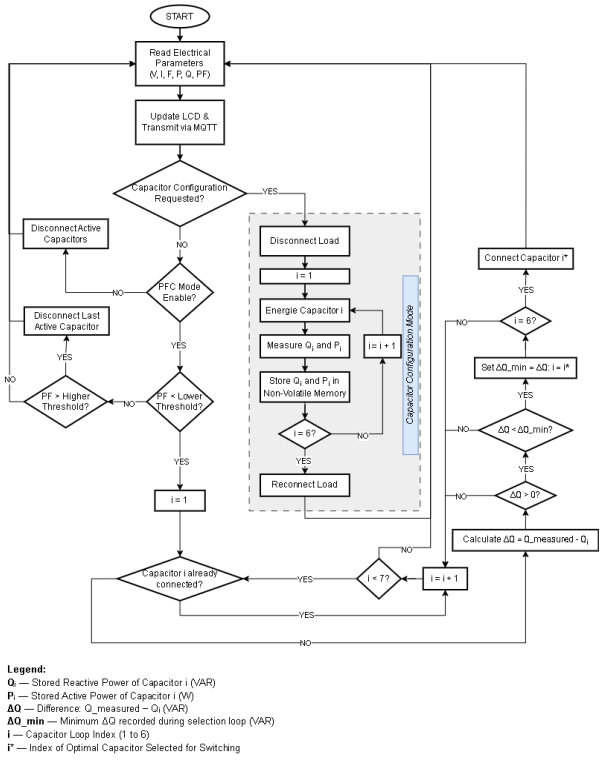

Fig. 2. Flowchart of the proposed APFC control algorithm.

E. User Interface and IoT Communication

A 20×4 LCD with PCF8574 I^2C interface displays continuously updated system measurements including voltage, current, active power, reactive power, power factor, and active capacitor steps. Three push buttons provide menu navigation and calibration mode access; a toggle switch enables manual activation or deactivation of the PFC mechanism. For wireless communication, the ESP32 connects to the HiveMQ MQTT broker via its internal Wi-Fi module, publishing measured electrical parameters to a dedicated topic. A custom mobile application developed using MIT App Inventor subscribes to this topic and presents real-time monitoring data to the end user.

IV. MATHEMATICAL MODELING

A. Single-Phase Power Relations

For a single-phase load operating at RMS voltage V and drawing RMS current I at phase angle φ between voltage and current, the three power quantities are defined as:

$$S = V \cdot I \quad (1)$$

$$P = S \cdot \cos\varphi \quad (2)$$

$$Q = S \cdot \sin\varphi \quad (3)$$

where S = apparent power (VA), P = active power (W), Q = reactive power (VAR), φ = phase angle.

Power factor is expressed as:

$$PF = \cos\varphi = P / S \quad (4)$$

Reactive power may also be written in terms of active power and power factor angle as:

$$Q = P \cdot \tan\varphi \quad (5)$$

B. Required Reactive Compensation

To improve power factor from an initial value $PF_1 = \cos\varphi_1$ to a target value $PF_2 = \cos\varphi_2$, the required compensating reactive power ΔQc is:

$$\Delta Qc = P(\tan\varphi_1 - \tan\varphi_2) \quad (6)$$

where P = active power of load (W), φ_1 = initial PF angle, φ_2 = target PF angle.

For the experimental test case, with P = 350 W, $PF_1 = 0.71$ ($\varphi_1 = 44.8°$), and target $PF_2 = 0.95$ ($\varphi_2 = 18.2°$), substituting into (6):

$$\Delta Qc = 350 \times (\tan 44.8° - \tan 18.2°) \approx 144 \text{ VAR} \quad (7)$$

C. Capacitor Sizing

The reactive power supplied by a shunt capacitor connected across a single-phase supply is:

$$Qc = V^2 \cdot 2\pi f \cdot C \quad (8)$$

where V = RMS supply voltage (V), f = supply frequency (Hz), C = capacitance (F).

Rearranging to obtain the required capacitance for a known compensation target:

$C = \Delta Qc / (2\pi f \cdot V^2)$ (9)

At V = 254.5 V and f = 50 Hz, the ideal per-step capacitor reactive contributions computed from (8) are: R1 (5.0 µF) ≈ 101.4 VAR; R2–R4 (2.5 µF each) ≈ 50.7 VAR; R5–R6 (1.5 µF each) ≈ 30.4 VAR. These values are stored in non-volatile memory during the capacitor characterization mode for use during real-time switching decisions.

D. Line Current Reduction

For a fixed active power load P, line current before and after compensation is:

$I_1 = P / (V \cdot PF_1)$ $I_2 = P / (V \cdot PF_2)$ (10)

Since $PF_2 > PF_1$, it follows that $I_2 < I_1$. The ratio of currents is:

$I_2 / I_1 = PF_1/PF_2 = \cos\varphi_1/\cos\varphi_2$ (11)

For the experimental case (PF_1 = 0.71, PF_2 = 0.97), the current ratio from (11) is 0.71/0.97 ≈ 0.732 representing a 26.8% reduction in line current after compensation.

E. Distribution Line Loss Reduction

Resistive distribution losses are proportional to the square of line current. For a feeder of resistance R:

$P_{loss} = I^2 \cdot R$ (12)

The percentage reduction in feeder losses achieved by power factor improvement is therefore:

Loss Reduction (%) = $[1 - (PF_1 / PF_2)^2] \times 100$ ...(13)

Substituting the experimental values into (13): Loss Reduction = $[1 - (0.71/0.97)^2] \times 100 \approx 46.4\%$. This confirms that distributed load-level compensation yields substantial reductions in feeder I^2R losses, validating the system's contribution to residential grid efficiency improvement.

V.EXPERIMENTAL SETUP

TABLE I. Experimental Components and Specifications

Component	Model / Specification	Qty.
Microcontroller	ESP32 DevKit V1, 240 MHz, Wi-Fi	1
Energy Monitor	PZEM-004T v4.0, 100 A	1
Current Transformer	Solid-core, non-contact (bundled with PZEM)	1
4-CH Relay Module	10 A / 250 VAC	1
2-CH Relay Module	10 A / 250 VAC	1
Load Isolation Relay	Single-channel, 30 A / 250 VAC	1
Capacitors	2.5 µF, 440 V AC, MPP type	5
Capacitors	1.5 µF, 440 V AC, MPP type	2
LCD Display	20×4, with PCF8574 I^2C interface	1
DC Power Supply	AC-DC adapter, 5 V / 2 A	1
User Interface	3× push buttons, 1× toggle switch, zero PCB	1
Isolation Switches	Rocker switches (supply, load, capacitor bank)	3
R Load	Incandescent filament bulb, 100 W / 230 V	1
R-L Load	100 W filament bulb + 43 W fluorescent choke ballast (parallel)	1

A. Test Bench Configuration

The prototype was assembled on a 6 mm plywood board housing all components in a compact, accessible layout. Three rocker switches provide independent isolation of the AC supply, load, and capacitor bank, allowing safe connection and disconnection of each subsystem during testing without disturbing the remaining circuitry. A 5 V / 2 A DC adapter supplies power to the ESP32, relay modules, LCD, and PZEM-004T logic circuitry. The experimental prototype is shown in Fig. 3.

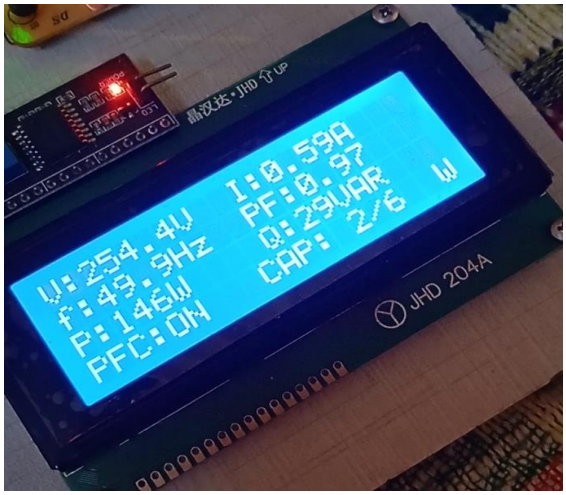

Fig. 3. Photograph of the assembled APFC experimental prototype.

B. Load Configurations

Two load configurations were tested. For the resistive load test, a single 100 W incandescent filament bulb was connected, representing a near-unity power factor baseline condition (PF ≈ 0.99–1.00) with no reactive demand. For the inductive load test, the same 100 W filament bulb was connected in parallel with a 43 W fluorescent choke ballast, producing a combined R-L load with a measured initial power factor of approximately 0.71 and a reactive power demand of approximately 141 VAR — representative of a typical residential inductive load scenario.

C. Experimental Procedure

Prior to testing, capacitor characterization mode was activated by toggling the designated switch. Each capacitor was individually energized, its actual reactive contribution measured by the PZEM-004T module, and the value stored in ESP32 non-volatile memory to account for component tolerances. During live testing, the system continuously acquired electrical parameters via UART, displayed real-time readings on the LCD, and executed the compensation algorithm autonomously. IoT functionality was verified by confirming live parameter updates on the MIT App Inventor mobile application subscribed to the designated HiveMQ broker topic. All measurements were recorded directly from the LCD display and the mobile application interface.

VI. RESULTS AND DISCUSSION

A. Resistive Load Test

Table II presents the measured electrical parameters under the purely resistive load condition. The system recorded a power factor of 0.99–1.00 with a negligible reactive power of approximately 5 VAR — consistent with the near-unity power factor characteristic of an incandescent filament load. The control algorithm correctly identified this condition as requiring no compensation and maintained all capacitor relays in the OFF state throughout the test. This confirms that the decision logic operates correctly under non-inductive conditions, preventing unnecessary reactive injection that would otherwise lead to a leading power factor.

TABLE II. Measured Parameters — Resistive Load

Parameter	Measured Value
RMS Voltage (V)	253.2 V
RMS Current (A)	0.40 A
Active Power (W)	100 W
Reactive Power (VAR)	≈ 5 VAR
Power Factor	0.99 – 1.00
Capacitor Steps Active	0 (all relays OFF)

B. R-L Load — Stepwise Compensation

Table III presents the experimental readings recorded during stepwise capacitor activation under the R-L load. At baseline (Step 0), the system measured a power factor of 0.71 with a reactive power demand of 141 VAR, confirming the need for compensation. Upon detection of this condition, the controller activated the first capacitor step (5.0 µF — two 2.5 µF capacitors in parallel via the 2-channel relay module), reducing reactive power from 141 VAR to 62 VAR and improving power factor to 0.90. A second step (additional 2.5 µF via the 4-channel relay module) further reduced reactive power to 29 VAR, achieving a final power factor of 0.97.

The controller correctly terminated switching at Step 2 verifying that the overcompensation prevention logic functioned as intended. Activating the next available step would have injected approximately 50 VAR into a system with only 29 VAR remaining reactive demand, resulting in a leading power factor condition. This demonstrates effective real-time decision-making under practical inductive loading.

TABLE III. Stepwise Compensation Results — R-L Load

Step	Capacitor Config.	V (V)	PF	Q (VAR)	Controller Action
0	No caps (baseline)	254.5	0.71	141	Compensation triggered

1	5.0 µF (Ch2, 2-CH relay)	254.5	0.90	62	Further step required
2	5.0 µF + 2.5 µF	254.5	0.97	29	Target reached — stopped

C. Theoretical vs. Experimental Comparison

Table IV and Figs. 1–2 compare the theoretical compensation values derived in Section IV with experimental measurements. At baseline, theoretical and experimental reactive power values differ by only 2.1% (144 VAR vs. 141 VAR), confirming the accuracy of the mathematical model under the given load conditions. At Step 1, a deviation of approximately 24% is observed in reactive power (50 VAR theoretical vs. 62 VAR experimental), attributed primarily to capacitor manufacturing tolerance (±5–10%), relay contact resistance, wiring impedance, and supply voltage fluctuation during switching. Correspondingly, the experimental power factor at Step 1 (0.90) is lower than the theoretical prediction (0.99). At Step 2, the experimental power factor of 0.97 closely approaches the theoretical near-unity value, confirming that cumulative compensation performance converges toward the predicted behavior.

TABLE IV. Theoretical vs. Experimental Comparison

Step	Theor. Q (VAR)	Expt. Q (VAR)	Q Dev. (%)	Theor. PF	Expt. PF
0 (baseline)	144	141	2.1%	0.71	0.71
1 (5.0 µF)	50	62	24.0%	0.99	0.90
2 (+2.5 µF)	≈ 0	29	—	≈ 1.00	0.97

Fig. 1. Reactive Power vs. Capacitor Steps (Theoretical vs. Experimental)

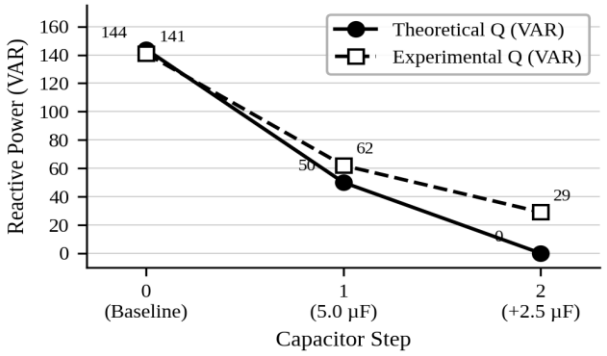

Fig. 2. Power Factor Improvement vs. Capacitor Steps (Theoretical vs. Experimental)

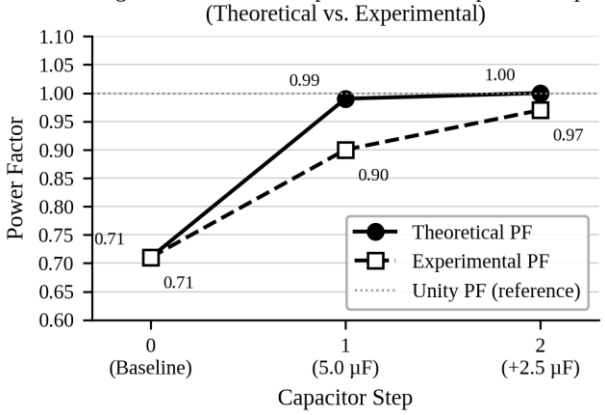

Fig. 1. Reactive power vs. capacitor steps — theoretical vs. Experimental.

D. Discussion

The experimental results confirm three key contributions of the proposed system. First, the APFC prototype successfully performed autonomous reactive power compensation under practical inductive loading, improving power factor from 0.71 to 0.97 — a 36.6% improvement — and reducing reactive power demand from 141 VAR to 29 VAR. Applying equation (13) from Section IV, this corresponds to an estimated 46.4% reduction in feeder I^2R losses, validating the system's contribution to residential distribution network efficiency.

Second, unlike conventional APFC prototypes that rely on pre-programmed or manually measured capacitor values, the proposed system incorporates an automated capacitor characterization mode that measures and stores each capacitor's actual reactive contribution under live supply conditions — eliminating manual calibration and enhancing consumer-side usability without requiring technical expertise. The accuracy of the compensation steps, which closely follow theoretical predictions, demonstrates the effectiveness of this self-characterization approach.

Third, real-time IoT monitoring was successfully demonstrated via MQTT communication through the HiveMQ broker, with live electrical parameters confirmed on the MIT App Inventor mobile application. This validates the system's compatibility with smart grid and AMI infrastructure requirements. The observed deviations between theoretical and experimental values within acceptable engineering tolerances are consistent with practical factors including capacitor aging, relay switching characteristics, and measurement uncertainty inherent to the PZEM-004T module (rated accuracy ±1%).

VII. CONCLUSION

This paper presented the design and experimental validation of a low-cost, IoT-enabled residential Automatic

Power Factor Correction (APFC) system utilizing an ESP32 microcontroller, PZEM-004T energy monitoring module, and a six-step relay-switched capacitor bank. The system successfully demonstrated autonomous reactive power compensation under practical inductive loading conditions, with experimental results closely corroborating theoretical predictions derived from the mathematical model. A key distinguishing contribution of the proposed prototype is its automated capacitor characterization mode, which measures and stores each capacitor's actual reactive contribution under live supply conditions — eliminating manual calibration and making the system genuinely accessible to non-technical residential users without any firmware modification.

Experimental validation confirmed a power factor improvement from 0.71 to 0.97, a reduction in reactive power demand from 141 VAR to 29 VAR, and an estimated 46.4% reduction in feeder I^2R losses — demonstrating meaningful potential for improving residential distribution network efficiency at scale. Real-time IoT monitoring via the Electrical Parameter Monitor (EPM) mobile application further validated the system's compatibility with smart grid and Advanced Metering Infrastructure requirements. Future work will focus on multi-unit coordination across residential feeders, integration with existing smart meter infrastructure, and evaluation under varying supply conditions and harmonic-rich load environments to assess scalability toward neighborhood-level deployment.

REFERENCES

[1] A. Á. Téllez, G. López, I. Isaac, and J. González, "Optimal Reactive Power Compensation in Electrical Distribution Systems with Distributed Resources: Review," Heliyon, vol. 4, no. 8, p. e00759, Aug. 2018.

[2] D. Stanelytė and V. Radziukynas, "Review of Voltage and Reactive Power Control Algorithms in Electrical Distribution Networks," Energies, vol. 12, no. 24, p. 4789, Dec. 2019.

[3] O. Candra, K. Hartmann, and N. Manthey, "Optimal Distribution Grid Allocation of Reactive Power with a Focus on the Particle Swarm Optimization Technique and Voltage Stability," Scientific Reports, vol. 14, no. 1, p. 10023, May 2024.

[4] T. Nguyen, A. Ngo, and L. Nguyen, "An Effective Reactive Power Compensation Method and a Modern Metaheuristic Algorithm for Loss Reduction in Distribution Power Networks," Complexity, vol. 2021, Article ID 6643210, Oct. 2021.

[5] S. Bolognani and S. Zampieri, "A Distributed Control Strategy for Reactive Power Compensation in Smart Microgrids," IEEE Transactions on Automatic Control, vol. 58, no. 11, pp. 2818–2833, Nov. 2013.

[6] M. Korchak, B. Savchyn, and O. Karpenko, "Virtual Source of Reactive Power in Electricity Supply Systems of Household Consumers," Energy Engineering and Control Systems, vol. 5, no. 1, pp. 19–25, Jan. 2019.

[7] M. Sarkar, J. Meegahapola, and M. Datta, "Reactive Power Management in Renewable Rich Power Grids: A Review of Grid-Codes, Renewable Generators, Support Devices and Optimization Algorithms," IEEE Access, vol. 6, pp. 41458–41489, May 2018.